



# Galaxy And Mass Assembly (GAMA): A “No Smoking” Zone for Giant Elliptical Galaxies?

Habib G. Khosroshahi<sup>1,2</sup>, Mojtaba Raouf<sup>1</sup>, Halime Miraghaei<sup>1</sup>, Sarah Brough<sup>3</sup>, Darren J. Croton<sup>4</sup>, Simon Driver<sup>5</sup>, Alister Graham<sup>4</sup>, Ivan Baldry<sup>6</sup>, Michael Brown<sup>7</sup>, Matt Prescott<sup>8</sup>, and Lingyu Wang<sup>9,10</sup>

<sup>1</sup> School of Astronomy, Institute for Research in Fundamental Sciences (IPM), Tehran, 19395-5746, Iran; [habib@ipm.ir](mailto:habib@ipm.ir)

<sup>2</sup> Institut d’Astrophysique de Paris, 98 bis Bd Arago, F-75014 Paris, France

<sup>3</sup> Australian Astronomical Observatory, P.O. Box 915, North Ryde, NSW 1670, Australia

<sup>4</sup> Centre for Astrophysics & Supercomputing, Swinburne University of Technology, P.O. Box 218, Hawthorn, Victoria 3122, Australia

<sup>5</sup> International Centre for Radio Astronomy Research (ICRAR), The University of Western Australia, 35 Stirling Highway, Crawley, WA 6009, Australia

<sup>6</sup> Astrophysics Research Institute, Liverpool John Moores University, IC2, Liverpool Science Park, 146 Brownlow Hill, Liverpool L3 5RF, UK

<sup>7</sup> School of Physics, Monash University, Clayton, VIC 3800, Australia

<sup>8</sup> Astrophysics Group, The University of Western Cape, Robert Sobukwe Road, Bellville 7530, South Africa

<sup>9</sup> SRON Netherlands Institute for Space Research, Landleven 12, 9747 AD, Groningen, The Netherlands

<sup>10</sup> Kapteyn Astronomical Institute, University of Groningen, Postbus 800, 9700 AV, Groningen, The Netherlands

Received 2017 February 16; revised 2017 April 6; accepted 2017 April 25; published 2017 June 15

## Abstract

We study the radio emission of the most massive galaxies in a sample of dynamically relaxed and unrelaxed galaxy groups from the Galaxy and Mass Assembly survey. The dynamical state of the group is defined by the stellar dominance of the brightest group galaxy (BGG), e.g., the luminosity gap between the two most luminous members, and the offset between the position of the BGG and the luminosity centroid of the group. We find that the radio luminosity of the largest galaxy in the group strongly depends on its environment, such that the BGGs in dynamically young (evolving) groups are an order of magnitude more luminous in the radio than those with a similar stellar mass but residing in dynamically old (relaxed) groups. This observation has been successfully reproduced by a newly developed semi-analytic model that allows us to explore the various causes of these findings. We find that the fraction of radio-loud BGGs in the observed dynamically young groups is  $\sim 2$  times that of the dynamically old groups. We discuss the implications of this observational constraint on the central galaxy properties in the context of galaxy mergers and the super massive black hole accretion rate.

*Key words:* galaxies: active – galaxies: elliptical and lenticular, cD – galaxies: groups: general

## 1. Introduction

An unresolved issue in extra-galactic astronomy is the heating of the inter-galactic medium (IGM) within the core of the galaxy groups and clusters, as gas in this region does not cool as dramatically as expected from the emitted X-ray emission (David et al. 2001; Peterson & Fabian 2006; McNamara & Nulsen 2007; Fabian 2012). Among the mechanisms proposed and discussed to balance the expected cooling, the role of active galactic nuclei (AGNs) feedback is seen as the most prominent (Blanton et al. 2010; Gaspari et al. 2011; Gitti et al. 2012), though the exact mechanisms are still debated. Mechanical heating (Bîrzan et al. 2004; Nulsen et al. 2007; Hlavacek-Larrondo et al. 2015), turbulence (Zhuravleva et al. 2014), mixing (Gilkis & Soker 2012), deposition of energy through AGN originated shocks (Graham et al. 2008; Randall et al. 2015), and sound waves (Fabian et al. 2006) are among the mechanisms through which the AGN could heat up the IGM in the group/cluster core. The evolution of galaxies and, in particular, the most massive galaxies in the universe are found in the core, which of groups and clusters, are clearly affected by AGN feedback (McNamara & Nulsen 2007), which is widely assumed in galaxy formation and evolution models (Croton et al. 2006).

In order to understand whether galaxy the environment influences AGN activity and thus feedback, we focus on dynamically relaxed galaxy groups also known as fossil groups (Ponman et al. 1994; Khosroshahi et al. 2004, 2007). The main characteristic of fossil groups is the stellar dominance of the brightest group galaxy (BGG), which is generally probed by the

optical luminosity or magnitude gap (e.g.,  $\Delta m_{12} \geq 2.0$ ) within the half-virial radius or in a fixed projected radius of the group halo (Jones et al. 2003). The conventional argument for the formation of fossil groups is based on a scenario in which a massive galaxy forms via cannibalizing its surrounding galaxies through dynamical friction, which requires several Gyr (Jones et al. 2000). A number of studies using cosmological simulations have shown that fossil galaxy group halos form relatively earlier than halos with a small luminosity gap (e.g.,  $\Delta m_{12} \leq 0.5$ ) and the results are consistent between hydrodynamical approaches (D’Onghia et al. 2005; Cui et al. 2011; Raouf et al. 2016) and semi-analytical models for galaxies (Dariush et al. 2007, 2010; Sales et al. 2007; Díaz-Giménez et al. 2008; Raouf et al. 2014). The observational findings appear to be consistent with the broad picture that groups with a large luminosity gap have an earlier formation epoch than those with a small luminosity gap (Khosroshahi et al. 2006, 2007; Smith et al. 2010).

AGNs are powered by gas accretion onto the super massive black hole at the center of galaxies. It has been argued that AGNs significantly affect the evolution of the host galaxy through quenching of the star formation and also that they affect the IGM heating through various feedback processes. The accretion of hot gas (Bondi accretion) is tightly correlated to the AGN jet power (Allen et al. 2006). Cold accretion (Werner et al. 2014) and black-hole spin (Russell et al. 2013) have also been explored to determine the main fueling mechanism. In a recent study of a small sample of fossil galaxy groups, we found indications that the most luminous galaxies in fossil galaxy groups, a representative for dynamically relaxed halos, are underluminous

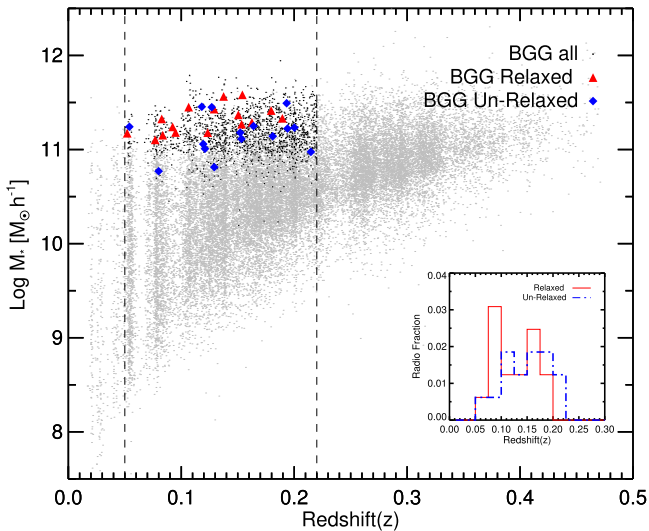


**Figure 1.** Selection function for the samples; the stellar mass of the BGGs as a function of the redshift. The background gray dots represent all galaxies assigned to groups in the entire GAMA database. The black dots represent luminous BGGs ( $M_r \leq -22$ ) within the redshift limit of the sample that is defined, based on the redshift completeness of the sample. The symbols represent BGGs in dynamically relaxed and unrelaxed groups with a radio detection in 1.4 GHz, with the subpanel representing their redshift distribution.

in radio emission in 610 MHz and 1.4 GHz (Miraghaei et al. 2014). This study suggests that mergers, the key phenomena behind the formation of a large luminosity gap, may be the main source of discrimination in the radio properties. In a more recent study we have examined the IGM heating sources in one of the most massive fossil groups (Miraghaei et al. 2015) and found that in the case of RX J1416.4+2315, the energy injected into the IGM by AGNs is only sufficient to heat up the central 50 kpc.

A number of studies found an increased fraction of AGNs in galaxies with close matches, ongoing mergers, or in post-merger systems (Ramos Almeida et al. 2011; Ellison et al. 2011; Bessiere et al. 2012; Cotini et al. 2013; Sabater et al. 2013). However, several studies claimed to find no significant excess of mergers in AGN hosts (Dunlop et al. 2003; Sanchez et al. 2004b; Grogin et al. 2005; Li et al. 2008; Gabor et al. 2009; Tal et al. 2009; Cisternas et al. 2011; Kocovski et al. 2012; Schawinski et al. 2012; Bohm et al. 2013). These studies report that a significant fraction of AGNs appear to reside in isolated disk-dominated galaxies for which internal processes are likely responsible for fueling their active nuclei. The focus of our study is on the brightest galaxies in the group, which are primarily giant elliptical galaxies. Assuming a simple picture for the gravitational collapse of gas into the center of a galaxy cluster, BCGs located at the cluster center will be influenced by a larger reservoir (density) of hot gas compared to BCGs with a large offset.

Galaxy groups in different dynamical states are suitable systems for the study of AGN fueling and its feedback on galaxy evolution, because of the absence of recent group scale mergers and galaxy major mergers in virialized groups compared to those of evolving groups (Jones et al. 2003). Although the luminosity gap and the offset between the BGG and the luminosity centroid are both indicators of the dynamical state/age of galaxy groups (Raouf et al. 2014), the luminosity gap is also a key player. The presence of a large luminosity gap points to the absence of a recent major merger, which could ignite the cold mode accretion, while an AGN at the bottom of the potential well

of the group/cluster, where the IGM reaches its peak density in a dynamically relaxed group, is subject to hot gas accretion. In Section 2 of this paper we describe the sample and the data. Section 3 is dedicated to the analysis, followed by a discussion and concluding remarks in Section 4.

Throughout this paper we use a  $\Lambda$ CDM cosmology with  $\Omega_m = 0.3$ ,  $\Omega_\Lambda = 0.7$ , and  $H_0 = 70 \text{ km s}^{-1} \text{ Mpc}^{-1}$ .

## 2. Data and Sample Selection

The main source of data for this study is the Galaxy And Mass Assembly (GAMA) survey, a multi-wavelength spectroscopic data set covering an area of  $180 \text{ deg}^2$ . The description of the survey is given in Baldry et al. (2010), while other aspects of the survey have been described in Robotham (2010), Driver et al. (2011), and Hopkins (2013). We use the second data release, GAMA-DRII.

We use the GAMA stellar masses catalog, which provides stellar masses, rest frame photometry, and other ancillary stellar population parameters from stellar population fits, to “ugriz” spectral energy distributions for all  $z < 0.65$  galaxies (Taylor et al. 2011).

The GAMA-DRII galaxy group catalog has been generated using a friends-of-friends based grouping algorithm (Robotham et al. 2011). The catalog contains 23,838 galaxy groups which reduce to about 2,500 galaxy groups and about 19,000 group members with a multiplicity of at least 4 spectroscopically confirmed members. Using the total extrapolate luminosity and the total stellar mass of the group galaxies and their positions, we obtain the luminosity gap and the luminosity centroid of the groups. We select a sample of dynamically relaxed galaxy groups and a control sample (dynamically evolving groups):

I. A sample of galaxy groups with a BGG at least as luminous as  $M_r = -22$  mag (total of 1533 groups) and with a large luminosity gap between the BGG and the second brightest group member,  $\Delta_{m_{12}} \geq 1.7$  in the r-band. In addition, we also impose that the BGG is located within a radius of 100 kpc of the luminosity/stellar-mass centroid of the group. This results in 174 groups.

II. A sample of galaxy groups with a BGG at least as luminous as  $M_r = -22$  mag and with a small luminosity gap,  $\Delta_{m_{12}} \leq 0.3$  in the r-band. We impose the BGG to be located outside the radius of 100 kpc, centered on the luminosity/stellar-mass centroid of the group. This results in 134 groups. We note that the majority of galaxy groups tend to have a small luminosity gap (Gozaliasl et al. 2014); however, the large offset requirement reduces the sample to a size comparable to that of Sample I.

The luminosity centroid of the group members is provided in the GAMA group catalog and is defined as the center of light derived from the r-band luminosity of all the galaxies identified to be within the group (Robotham et al. 2011). The redshift limit is chosen on the basis of providing a complete sample of groups with a luminosity gap of 1.7 mag. We cross-match the BGGs with the VLA FIRST catalog of objects detected in 1.4 GHz. The FIRST survey released a catalog that contains all the radio sources detected above a limiting flux density of  $\sim 1$  mJy for point sources with a typical noise of  $\sigma \sim 0.13$  mJy (Becker et al. 1995). About 10% of the luminous BGGs ( $M_r \leq -22$ ) in the sample are associated with a FIRST catalog source. Among the radio-detected BGGs, about 10% are assigned to relaxed groups and an equal fraction are assigned to unrelaxed groups, with a redshift distribution shown in the subpanel in Figure 1. The focus of the study will be on the

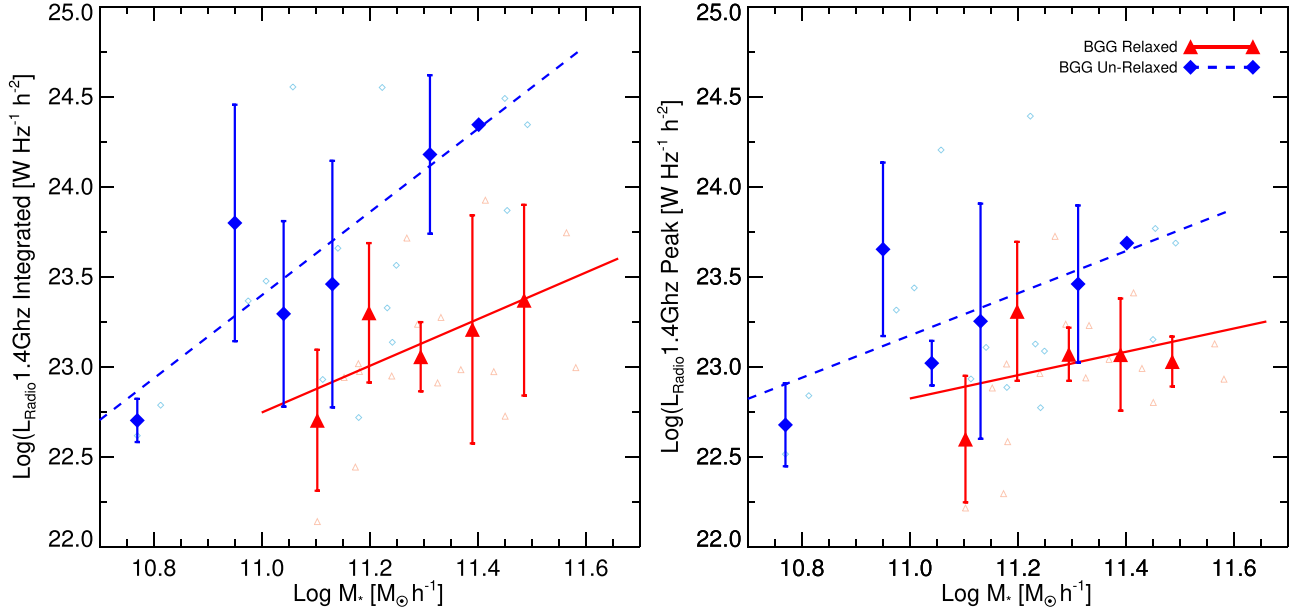


**Figure 2.** 1.4 GHz radio power of the BGG in old or dynamically relaxed groups (red) and young or evolving groups (blue). Old galaxy groups are selected to have a large luminosity gap ( $\Delta m_{12} \geq 1.7$ ) and a relatively small offset between the BGG and the luminosity centroid of the group ( $\leq 100$  kpc). Young groups have small luminosity gaps ( $\Delta m_{12} \leq 0.3$ ) and a large offset ( $\geq 100$  kpc). The radio luminosity refers to the integrated (left) and peak (right) flux densities obtained from the VLA FIRST catalog. The bold symbols mark the median value over the bin (0.1 in log scale) and the small symbols represent individual BGGs. The scatter is also shown for the binned data. The solid/dashed lines indicate linear regressions to the binned data.

**Table 1**  
Sample of BGGs in Dynamically Relaxed Galaxy Groups

| GroupID<br>GAMA-ID | R.A.<br>(deg) | Decl.<br>(deg) | $\Delta m_{12}$<br>(mag) | $D_{\text{off-centr}}$<br>(kpc) | $\text{Log}(L_{\text{int}})_{1.4 \text{ GHz}}$<br>( $\text{W Hz}^{-1} h^{-2}$ ) | $\text{Log}(L_{\text{peak}})_{1.4 \text{ GHz}}$<br>( $\text{W Hz}^{-1} h^{-2}$ ) | $\text{Log}(L)_{325 \text{ MHz}}$<br>( $\text{W Hz}^{-1} h^{-2}$ ) | $\text{Log}(M_{\text{halo}})$<br>( $M_{\odot}$ ) |
|--------------------|---------------|----------------|--------------------------|---------------------------------|---|--|--|--|
| 300395             | 214.64665     | -0.68262       | 2.5                      | 52.5                            | 22.98   | 23.04  | 23.79 <sup>†</sup>   | 12.75  |
| 200594             | 179.98355     | -0.32312       | 2.2                      | 24.5                            | 22.94   | 22.88  | 23.24 <sup>†</sup>   | 13.97  |
| 300260             | 214.45775     | 0.51094        | 1.8                      | 78.2                            | 22.44   | 22.30  | no detection   | 14.66  |
| 300422             | 216.4731      | 0.5803         | 1.7                      | 77.9                            | 22.97   | 22.99  | 23.64 <sup>†</sup>   | 13.97  |
| 200204             | 176.83746     | -1.70279       | 2.8                      | 20.7                            | 22.95   | 22.96  | 23.52  | 14.80  |
| 200122             | 176.79744     | -1.88907       | 1.8                      | 52.6                            | 22.97   | 22.58  | 22.81 <sup>†</sup>   | 14.28  |
| 100172             | 140.3522      | -0.40958       | 1.9                      | 58.3                            | 22.99   | 22.93  | 23.81 <sup>†</sup>   | 14.62  |
| 300083             | 219.16068     | 1.18301        | 3.0                      | 91.2                            | 23.74   | 23.13  | 24.07  | 13.90  |
| 300282             | 219.69284     | 1.11603        | 2.4                      | 61.2                            | 22.91   | 22.94  | 23.22 <sup>†</sup>   | 15.68  |
| 200524             | 178.85081     | 1.96747        | 2.2                      | 66.1                            | 23.92   | 23.41  | no detection   | 14.02  |
| 200873             | 180.59833     | 1.87271        | 1.9                      | 46.4                            | 23.24   | 23.24  | no detection   | 13.34  |
| 300874             | 216.37852     | 1.93393        | 1.9                      | 50.3                            | 23.71   | 23.72  | 23.81 <sup>†</sup>   | ...*   |
| 300542             | 215.39764     | 1.38464        | 1.7                      | 85.6                            | 23.27   | 23.23  | 24.01 <sup>†</sup>   | 13.72  |
| 300390             | 213.25523     | -1.1241        | 2.5                      | 29.7                            | 22.14   | 22.22  | 23.16 <sup>†</sup>   | 13.40  |
| 301140             | 217.60904     | -1.13174       | 1.8                      | 57.3                            | 23.02   | 23.02  | 23.60 <sup>†</sup>   | 14.13  |
| 200025             | 175.44472     | -0.51805       | 2.3                      | 84.5                            | 22.73   | 22.80  | 23.46 <sup>†</sup>   | 13.86  |

**Note.** The upper limit of 325 MHz luminosity for undetected sources is marked with the <sup>†</sup> signs. Note that the group's halo mass is not reported by the GAMA group catalog (see, Robotham et al. 2011). (\*)

BGGs hosted by relaxed and unrelaxed groups with a detected radio emission. The low-frequency radio emission at 325 MHz has been obtained for the GAMA fields using GMRT observations (Mauch et al. 2013) with 14–24 arcsec resolution and  $\sim 10$  mJy limiting flux density. The low-frequency observations allow us to study low-energy electrons and thus, the past AGN activities of galaxies (Miraghaei et al. 2014).

Figure 1 shows the selection function of the sample highlights, the stellar mass of the BGGs, and the redshift distribution of the groups (e.g., the redshift associated with the BGG). The small difference between the adopted  $\Delta m_{12} = 1.7$

limit used for the selection of the relaxed groups and the one conventionally used in previous studies of fossil groups,  $\Delta m_{12} = 2.0$ , is to ensure a statistically meaningful number of galaxies in both the above samples. Other authors have also adapted similar variations in the sample selection of fossil galaxy groups (e.g., Gozaliasl et al. 2014).

### 3. Analysis and Results

We first attempt to establish whether the ongoing AGN activity in the BGGs probed by the 1.4 GHz luminosity is influenced by the dynamical state of the group, based on the

**Table 2**  
Sample of BGGs in Dynamically Unrelaxed (Evolving) Galaxy Groups

| GroupID<br>GAMA-ID | R.A.<br>(deg) | Decl.<br>(deg) | $\Delta m_{12}$<br>(mag) | $D_{\text{off-centr}}$<br>(kpc) | $\text{Log}(L_{\text{int}})_{1.4 \text{ GHz}}$<br>( $\text{W Hz}^{-1} h^{-2}$ ) | $\text{Log}(L_{\text{peak}})_{1.4 \text{ GHz}}$<br>( $\text{W Hz}^{-1} h^{-2}$ ) | $\text{Log}(L)_{325 \text{ MHz}}$<br>( $\text{W Hz}^{-1} h^{-2}$ ) | $\text{Log}(M_{\text{halo}})$<br>( $M_{\odot}$ ) |
|--------------------|---------------|----------------|--------------------------|---------------------------------|---|--|--|--|
| 100046             | 140.65239     | -0.40903       | 0.2                      | 159.4                           | 23.13   | 22.77  | 23.45  | 13.88  |
| 200565             | 178.36423     | -1.18102       | 0.2                      | 144.0                           | 22.62   | 22.51  | 24.02  | 12.22  |
| 200043             | 184.70724     | -1.04693       | 0.1                      | 153.7                           | 23.87   | 23.77  | 24.29  | 14.69  |
| 300170             | 222.57996     | -1.11318       | 0.1                      | 280.9                           | 24.55   | 24.20  | no detection   | 13.69  |
| 300102             | 213.46605     | -0.6308        | 0.3                      | 149.6                           | 23.47   | 23.44  | 23.58 <sup>†</sup>   | 13.85  |
| 300033             | 213.73576     | 0.20641        | 0.1                      | 119.4                           | 24.48   | 23.15  | 24.74  | 14.17  |
| 301202             | 216.47969     | -0.27155       | 0.2                      | 202.2                           | 22.78   | 22.84  | 23.64 <sup>†</sup>   | 13.59  |
| 200435             | 185.30832     | -1.37898       | 0.0                      | 101.6                           | 22.72   | 22.88  | 23.80 <sup>†</sup>   | 13.84  |
| 200045             | 180.76495     | -1.93058       | 0.1                      | 200.8                           | 22.93   | 22.93  | 23.80 <sup>†</sup>   | 13.97  |
| 100079             | 137.97845     | 1.14878        | 0.1                      | 267.6                           | 23.56   | 23.09  | 24.76  | 14.32  |
| 300377             | 213.06422     | -1.13354       | 0.0                      | 356.8                           | 23.66   | 23.11  | 23.96  | 13.53  |
| 200022             | 183.08499     | 1.80787        | 0.1                      | 272.3                           | 24.34   | 23.68  | no detection   | 14.18  |
| 300392             | 213.03886     | -0.83542       | 0.2                      | 159.2                           | 24.55   | 24.39  | 24.90  | 13.19  |
| 100286             | 131.20869     | 1.60518        | 0.1                      | 168.2                           | 23.33   | 23.13  | 24.46  | 13.59  |
| 301381             | 214.6561      | 1.65797        | 0.1                      | 149.6                           | 23.37   | 23.31  | 24.13 <sup>†</sup>   | 12.84  |

**Note.** The upper limit of 325 MHz luminosity for the undetected sources is marked with <sup>†</sup> signs.

**Table 3**

The Slope and Intercept ( $a$  and  $b$ ) of the Radio Luminosity—Stellar-mass Relation for Our Samples

| Group  | $a$              | $b$               | Count           |
|--|------------------|-------------------|-----------------|
| Relaxed (1.4 GHz integrated)                     | $1.47 \pm 0.76$  | $6.55 \pm 8.54$   | 16              |
| Unrelaxed (1.4 GHz integrated)                   | $2.45 \pm 0.75$  | $-3.65 \pm 8.38$  | 15              |
| Relaxed (1.4 GHz peak)                           | $0.65 \pm 0.91$  | $15.69 \pm 10.26$ | 16              |
| Unrelaxed (1.4 GHz peak)                         | $1.17 \pm 0.6$   | $10.28 \pm 6.68$  | 15              |
| Relaxed (325 MHz)                                | $1.71 \pm 0.0^*$ | $4.29 \pm 0.0^*$  | 13 <sup>†</sup> |
| Unrelaxed (325 MHz)                              | $0.7 \pm 0.95$   | $16.52 \pm 10.7$  | 13              |
| Fossil ( $\Delta m_{12} > 1.7$ )                 | $1.08 \pm 0.21$  | $10.87 \pm 2.39$  | 29              |
| Non-fossil ( $\Delta m_{12} < 0.3$ )             | $0.46 \pm 0.53$  | $18.08 \pm 5.88$  | 23              |
| Low off-   | $0.6 \pm 0.36$   | $16.65 \pm 3.97$  | 65              |
| set ( $D_{\text{off-centr}} < 100 \text{ kpc}$ ) |                  |                   |                 |
| High off-  | $0.98 \pm 0.30$  | $12.26 \pm 3.34$  | 73              |
| set ( $D_{\text{off-centr}} > 100 \text{ kpc}$ ) |                  |                   |                 |
| Old (SAM)  | $3.2 \pm 0.08$   | $-12.97 \pm 0.86$ | 2515            |
| Young (SAM)                                      | $2.43 \pm 0.11$  | $-3.63 \pm 1.23$  | 458             |

**Note.** (\*) Note the limited statistics. (<sup>†</sup>) marks an upper limit.

two aforementioned halo age indicators, the luminosity gap, and the BGG offset. The observed correlations between the masses of black holes in the nuclei of nearby galaxies and global galactic properties, as the bulge luminosity or the central velocity dispersion, point toward a direct link between the physical processes that contribute to the central black hole's growth and the formation of their host galaxies.

In Figure 2 we present the distribution of the BGG radio emission as a function of the galaxy stellar mass for the two samples. We quantify the relation between the radio luminosity and the stellar mass of the BGG using a linear regression,  $\log(L_{\text{radio}}) = a(\log(M_{*})) + b$ , where  $a$  and  $b$  are given in Table 1 for the different samples. This is a clear demonstration that the relaxed (old) galaxy groups harbor BGGs that are less radio luminous in comparison to BGGs in groups that are classified as unrelaxed or evolving (young). The difference in the radio luminosity of the BGGs in these two dynamically different environments is measured to be a striking 1 order of magnitude in the radio luminosity, pointing to a significant, if

not determining, influence of the environment of the AGN activities in the BGGs. The results are the same when we adapt both the peak and the integrated-radio luminosity at the location of the BGGs.

We argue that this is not an observational bias. For instance, the source confusion may be seen as a possible reason for the observed difference. If the radio luminosities of two or more galaxies in the sample with the least luminosity gap are attributed to the BGG due to poor angular resolution, the BGGs in the sample of evolving groups will appear over-luminous in the radio. The spatial resolution of the VLA FIRST is  $\leq 5$  arcsec. For the most distant group sample at a redshift of  $\approx 0.3$ , such an angular resolution corresponds to a physical size of  $\approx 20$  kpc. To eliminate any such source confusion bias, both samples are required to have at least a 60 kpc projected separation between the two most luminous galaxies. It is clear that, given the definition of the samples described above, this additional criteria will only affect the statistics in Sample II. However, this is a small effect and Samples I and II contain 16 and 15 BGGs, respectively. The two samples are presented in Tables 1 and 2. We use both the peak radio luminosity and the integrated radio luminosity in our comparisons to rule out such a bias. The visual inspection shows no indication of source confusion. This is an additional constraint on Samples I and II that is described in Section 2, with the final statistics presented in Table 3. We note that this 60 kpc cut between the two most luminous galaxies in the groups is different from the 100 kpc offset between the BGG and the group luminosity centroid.

### 3.1. Luminosity Gap versus Off-centering

While we have established that the BGGs in relaxed galaxy groups are strikingly underluminous in radio continuum emission in comparison to those hosted by evolving groups, we now explore the origin of the observed difference. In particular, we attempt to discriminate between the effect of galaxy mergers, which are the driving phenomena behind the formation of the large luminosity gap, and the role of the hot mode accretion, which may be occurring given the privileged position of the BGG at the bottom of the potential well, where gas accretion is expected to be directed toward. We recognize

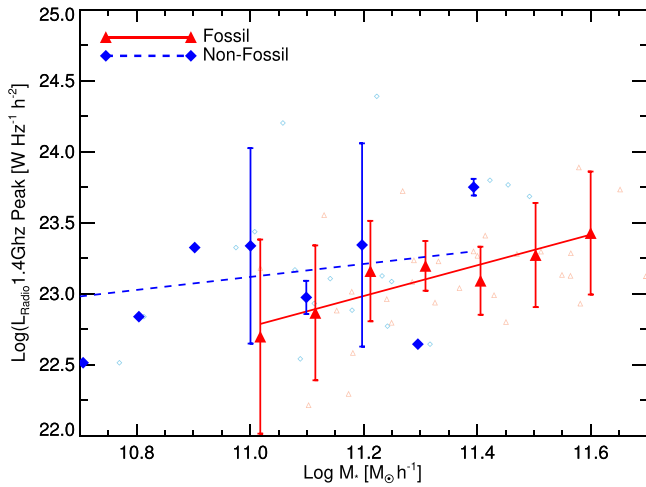


**Figure 3.** 1.4 GHz radio power of the BGG in fossil groups ( $\Delta m_{12} \geq 1.7$ , red) and non-fossil groups ( $\Delta m_{12} \leq 0.3$ , blue). The radio luminosity refers to the peak flux density obtained from the VLA FIRST catalog. The bold and small symbols refer to the average bin and the individual BGGs, respectively.

that X-ray observations are not featured in our study, however, a recent study by Khosroshahi et al. (2014) has shown that under a similar selection criteria employed in this study, an extended X-ray emission, associated with the group halo, surrounds the giant elliptical galaxy.

We thus relax the offset criterion for the BGG and only keep the constraint on the luminosity gap in both samples. The difference between the radio luminosity of the BGGs in large and small luminosity gap groups is significantly reduced and thus the BGGs in large luminosity gap systems, conventionally known as fossil groups, are marginally less luminous in the radio (Figure 3) than in the control sample in which the luminosity gap is very small. Thus, the cold mode accretion due to mergers does not appear to be the driving phenomena behind the observed difference in the radio luminosity of the BGGs in the two samples and as a result, their AGN activities.

We relax the luminosity gap criterion to study the role of the offset between the BGG and the luminosity centroid of the galaxies in order to find out if a large centroid offset, which can disrupt the hot mode accretion onto the central galaxy, plays a role in the AGN activity. Figure 4 shows that such an offset does not influence the BGG radio luminosity. We note that both the small number statistics and the absence of X-ray data are two limiting factors in making a concrete statement on the influence of the BGG position within the group and its radio activity. It is worth noting that Sanderson et al. (2009), in a study of a sample of galaxy clusters, found that the BGGs that are located within 15 kpc of the peak of the X-ray emission are more likely to be associated with the radio and line emission than those that show a larger centroid offset from the cluster core, which contradicts our findings in Figure 4; however, the offset scale used in this study is larger.

### 3.2. The Radio Map

We visually inspected the radio map of these galaxies in the two categories. Roughly, 5% of both samples have radio emission above  $3\sigma$  as shown in Figures 5 and 6. The radio contours in 1.4 GHz from the VLA survey (Becker et al. 1995) are overlaid on the optical images of the groups from the Sloan

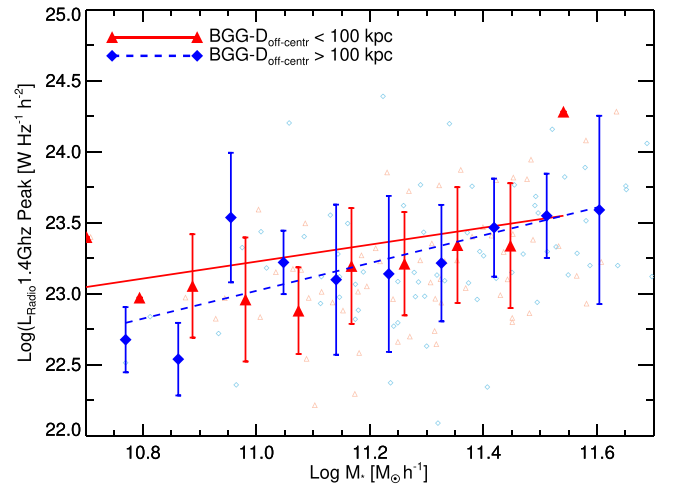


**Figure 4.** 1.4 GHz radio power of the BGG in groups with a small off-centering between the BGG position and the luminosity centroid of the group ( $\leq 100$  kpc, red) and large off-center groups ( $\geq 100$  kpc, blue). The radio luminosity refers to the peak flux density obtained from the VLA FIRST catalog. No significant difference between the radio power of the BGGs is seen in the two samples. The bold and small size symbols refer to the average bin and the individual BGGs, respectively.

Digital Sky Survey data release 12 (Alam et al. 2015, SDSS-DR12) archive.

The radio contours of young evolving groups show the existence of both extended and point source emission, while nearly all BGGs dominating relaxed galaxy groups show no extended emission. Single or double radio lobes have been detected in about 30% of the unrelaxed group sample compared to 10% for the relaxed group samples. The fraction of BGGs with radio-loud AGNs ( $L_{\text{radio}} \geq 10^{23} \text{ W Hz}^{-1}$ ) is 73% in young systems, while it is only 37% in relaxed groups.

Furthermore, we adapted the 325 MHz GMRT radio luminosity to investigate the low-frequency radio emission of the BGGs in relaxed and unrelaxed samples and the results are presented in Figure 7. The young (filled blue) and old (filled red) samples have been cross-matched with the 325 MHz GMRT observations of the GAMA field (Mauch et al. 2013) within a 1 arcmin search radius. Given the sensitivity of the 325 MHz map, fewer objects have been detected in 325 MHz, consisting of 2 and 7 objects in the old and young samples, respectively. Thus, we also present an upper limit luminosity for the undetected objects in 325 MHz in Figure 7 (open markers) in which we used the 10 mJy flux density limit to calculate the luminosities. This further supports the results based on the 1.4 GHz measurements where the BGGs in old groups are less luminous compared to those in the young evolving galaxy groups. As the plot indicates, we find a higher fraction of radio-loud sources among the BGGs in young evolving groups than in the old and relaxed galaxy groups. Only 7% of the BGGs in old systems show radio emission above  $L_{325 \text{ MHz}} \geq 10^{24} \text{ W Hz}^{-1}$ , while 46% of BGGs in young groups have emission above this luminosity.

We limit our analysis to BGGs that are at least as bright as  $M_R < -22$  mag to avoid late-type modest galaxies, i.e., targeting the giant galaxies in both samples of relaxed and unrelaxed. However, two of the BGGs in the relaxed galaxy groups and one BGG in the unrelaxed galaxy groups are morphologically classified as spirals.

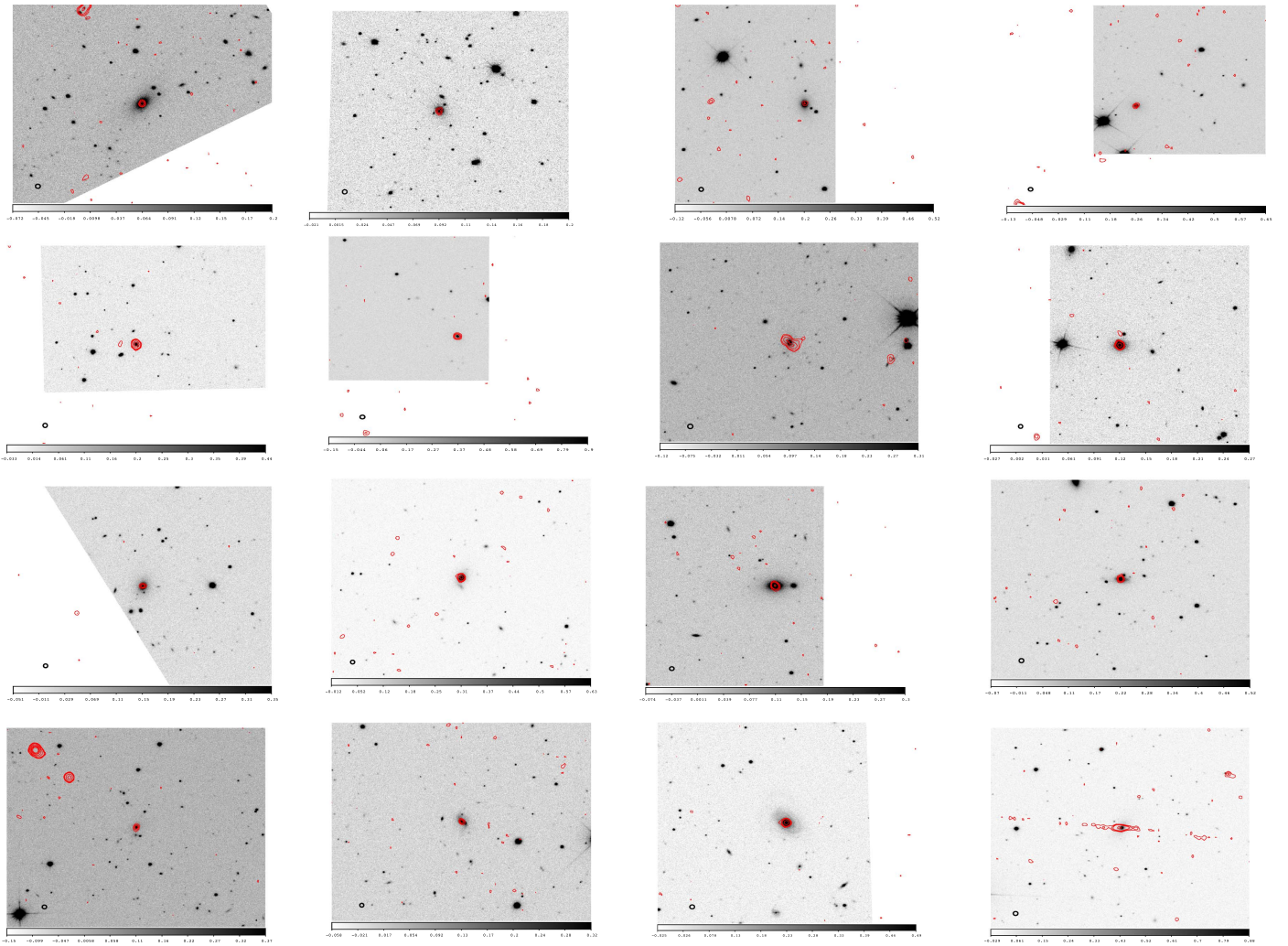


**Figure 5.** Radio contours overlaid on an SDSS r-band image for relaxed (red) groups. Contour levels of 3, 5, 7, 19, 40, 80, 120, 180, 300, 500, 800, and  $1000\sigma$  are shown. The rms noise ranges from 0.1 to 0.2 mJy in the sample.

### 3.3. Semi-analytic Prediction

The observational results described above are highly significant for understanding the AGN properties and their impact on galaxy evolution and environment dependent feedback. Given this, our efforts were focused on modeling the radio AGN in a cosmological context using the SAGE semi-analytic galaxy model (Croton et al. 2016) and the Millennium Simulation (Springel et al. 2005). We developed a new method in which we trace the physical properties of radio jets in massive galaxies, including the evolution of radio lobes and their impact on the surrounding gas. In our model, we self-consistently trace the cooling-heating cycle that significantly shapes the life and death of many types of galaxies (Radio-SAGE; Raouf et al. 2017). As the development of this model was motivated by the observations described above, the radio luminosity, as an observable quantity, is calculated to allow us to study the effect of environment on the AGN radio luminosity, the radio luminosity function, and the properties of jet power in the formation of host galaxies.

For a comparison of our observational results with the model prediction, we select dynamically relaxed and unrelaxed galaxy groups in our semi-analytic model on the basis of their mass assembly. According to Raouf et al. (2014), the groups are classified as dynamically relaxed (old) and unrelaxed (young)

when the halos accumulated  $>50\%$  and  $<30\%$  of their final mass at  $z \sim 1$ , respectively. Figure 8 shows the BGG peak and integrated radio luminosity (at 1.4 GHz) as a function of their stellar mass, in comparison to Figure 2. Both the observed data and the model predictions are shown in the figures. For the calibration of the model luminosity we used the Best & Heckman (2012) catalog of radio galaxies, which extends to  $z = 0.7$ .

Given that the jet power in radio galaxies directly correlates with the accretion rate of the super massive black hole, the consistency between observations and model predictions suggests a higher rate of accretion for the central black hole hosted by the most massive galaxy in dynamically evolving (young) galaxy groups relative to those hosted by dynamically evolved (old) galaxy groups at a given stellar mass.

These findings also agree with a recent study of galaxy groups in the Illustris hydrodynamical simulation (Vogelsberger et al. 2014), in which we found a lower rate of black hole accretion for a given stellar mass of the BGGs in comparison to those of the BGGs in young galaxy groups (Raouf et al. 2016).

## 4. Discussion and Conclusions

Using a sample of galaxy groups from the GAMA survey, we demonstrate that the radio luminosity of the most luminous

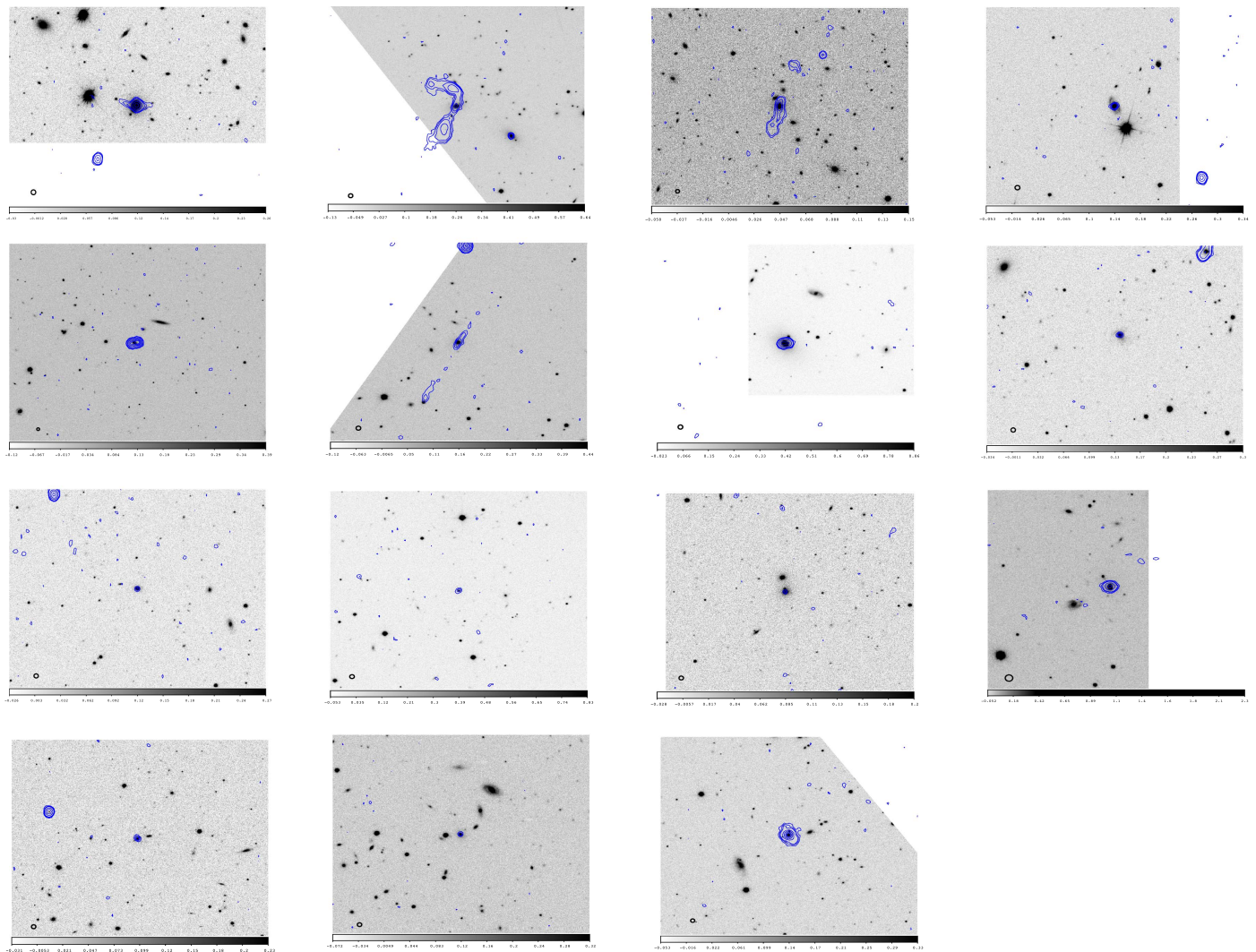


**Figure 6.** Radio contours overlaid on an SDSS r-band image for evolving or unrelaxed (blue) groups. Contour levels of 3, 5, 7, 19, 40, 80, 120, 180, 300, 500, 800, and 1000 $\sigma$  are shown. The rms noise ranges from 0.1 to 0.2 mJy in the sample.

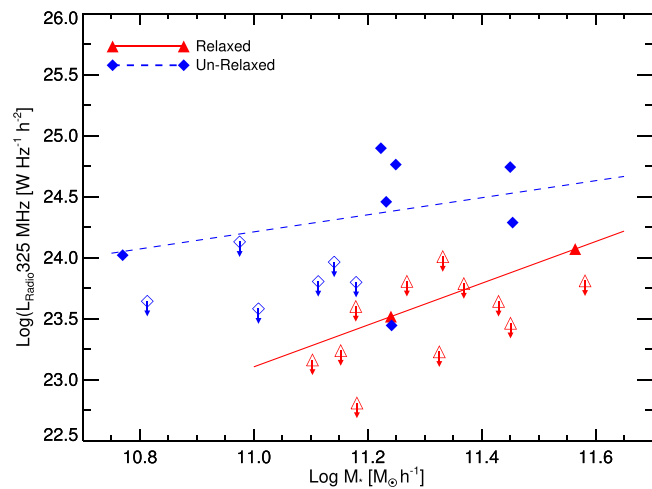


**Figure 7.** 325 MHz radio power of the BGGs in relaxed (filled red) and unrelaxed (filled blue) groups. An upper limit is given for the undetected relaxed (open red) and unrelaxed (open blue) BGGs. The majority of BGGs in dynamically relaxed groups are radio-loud.

galaxies, usually found in the cores of galaxy groups and clusters, and hence their AGN activities, depends on the dynamical state of the halo. We used two independent indicators to probe the dynamical state of the halo. The luminosity gap is expected to develop as a result of the internal mergers within groups, as argued in the formation of fossil galaxy groups and as shown in the cosmological simulations. We found no strong observational support to suggest that the AGN activity in the BGGs crucially depends on the luminosity gap alone evidently, AGN activity stems from major mergers between galaxies in groups. The merger galaxies finding may seem to be in conflict with a recent study of the BGGs in 610 MHz and 1.4 GHz, which points at a similar difference in the radio luminosity of the BGGs in the fossil and other galaxy groups (Miraghaei et al. 2014). However, its important to note that the sample that later study satisfies the large luminosity gap criterion explicitly, but it also satisfies the small BGG offset criterion implicitly, because the BGGs are located at the peak of the X-ray emission. Therefore, the small sample studied by Miraghaei et al. (2014) can be classified as dynamically relaxed

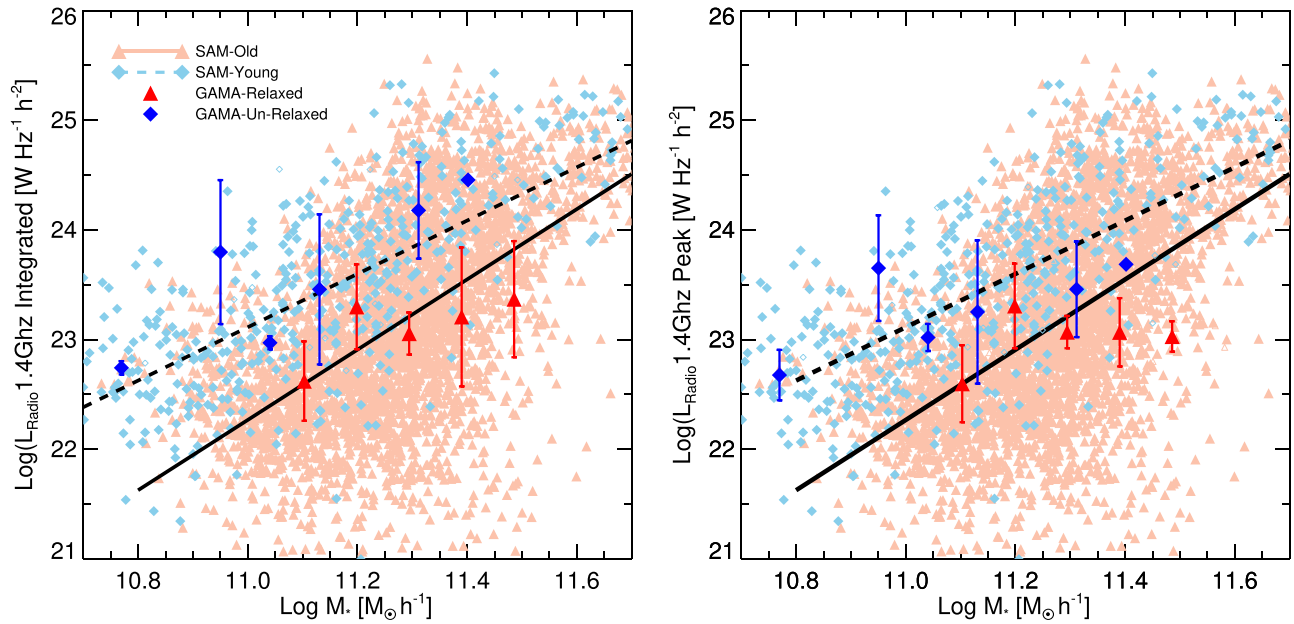


**Figure 8.** 1.4 GHz radio power of the BGG in old or dynamically relaxed groups (red) and young or evolving groups (blue), following Figure 2. The radio luminosity refers to the integrated (left) and peak (right) flux densities obtained from the VLA FIRST catalog. The bold symbols indicate the average value over the bin. We overlay the central galaxies in old (light red triangles) and young (sky blue diamonds) galaxy groups corresponding to different stellar masses as a function of the radio luminosity predicted by our galaxy formations model. The solid and dashed-lines represent linear fits to the model data points for the BGGs in old and young galaxy groups, respectively.

groups, according to this study. A more recent study of the IGM properties in fossil groups based on *Chandra* X-ray observations shows that the majority of the fossils harbor weak cool-cores (Bharadwaj et al. 2016). This confirms our earlier findings on the IGM temperature within the core of the fossil groups (Khosroshahi et al. 2004, 2007) and the absence of strong cool-cores in fossils. This study rules out current/strong AGN activities in fossil group dominant galaxies.

The most plausible explanation for our results is that while recent major mergers could be one of the driving phenomena behind the reduced AGN fueling, the dynamical state of the group, e.g., the combination of the large luminosity gap and the virialization of the halo, is the key driver behind the observed lack of AGN activity probed by the radio emission. Tracing the evolution of the dynamically relaxed halos in the cosmological simulations (Raouf et al. 2014) suggests that their BGGs had their last major merger relatively earlier than the BGGs in the unrelaxed groups. An alternative explanation would be the lack of inherent gas in the BGGs within the large luminosity gap groups; however, there is no evidence from the morphological or star formation history of the BGGs to support this argument. The BGGs in relaxed or unrelaxed groups are likely to be equally influenced by minor mergers.

We developed a semi-analytic model for radio AGNs to understand the origin of the observed trend. Our model has been able to reproduce the observed offset in the radio luminosity of the BGGs in dynamically relaxed and unrelaxed groups to a large extent. Our interpretation of the results is that the super massive black hole hosted by the BGGs in dynamically young galaxy groups is subject to a higher rate of accretion for the same stellar-mass budget than those of the BGGs in dynamically old galaxy groups.

We conclude that neither the offset between the position of the BGGs and the luminosity centroid of the group members, nor the large luminosity gap alone, can be responsible for the large radio luminosity offset between the BGGs in dynamically relaxed and unrelaxed galaxy groups. Together they conspire to

conceive the observed offset and thus the observed effect is driven by the difference in both the hot and cold accretion modes.

We thank the anonymous referee for the constructive comments and suggestions, which helped to improve the manuscript. GAMA is a joint European-Australasian project based around a spectroscopic campaign using the Anglo-Australian Telescope. The GAMA input catalog is based on data taken from the Sloan Digital Sky Survey and the UKIRT Infrared Deep Sky Survey. Complementary imaging of the GAMA regions is obtained by a number of independent survey programs including *GALEX* MIS, VST KiDS, VISTA VIKING, WISE, Herschel-ATLAS, GMRT, and ASKAP, providing UV to radio coverage. GAMA is funded by the STFC (UK), the ARC (Australia), the AAO, and the participating institutions. The GAMA web site is <http://www.gama-survey.org/>. The Radio Semi-Analytic Galaxy Evolution (Radio-SAGE) model used in this study is a publicly available for download at <https://github.com/mojtabaraouf/sage>. The Millennium Simulation was carried out by the Virgo Supercomputing Consortium at the Computing Centre of the Max Plank Society in Garching.

## References

- Alam, S., Albareti, F. D., Allende Prieto, C., et al. 2015, *ApJS*, **219**, 12  
 Allen, S. W., Dunn, R. J. H., Fabian, A. C., Taylor, G. B., & Reynolds, C. S. 2006, *MNRAS*, **372**, 21  
 Baldry, I. K., Robotham, A. S. G., Hill, D. T., et al. 2010, *MNRAS*, **404**, 86  
 Becker, R. H., White, R. L., & Helfand, D. J. 1995, *ApJ*, **450**, 559  
 Bessiere, P. S., Tadhunter, C. N., Ramos Almeida, C., & Villar Martín, M. 2012, *MNRAS*, **426**, 276  
 Best, P. N., & Heckman, T. M. 2012, *MNRAS*, **421**, 1569  
 Bharadwaj, V., Reiprich, T. H., Sanders, J. S., & Schellenberger, G. 2016, *A&A*, **585**, A125  
 Birzan, L., Rafferty, D. A., McNamara, B. R., Wise, M. W., & Nulsen, P. E. J. 2004, *ApJ*, **607**, 800

- Blanton, E. L., Clarke, T. E., Sarazin, C. L., Randall, S. W., & McNamara, B. R. 2010, *PNAS*, **107**, 7174
- Bohm, A., Wisotzki, L., Bell, E. F., et al. 2013, *A&A*, **549**, A46
- Cisternas, M., Jahnke, K., Inskip, K. J., et al. 2011, *ApJ*, **726**, 57
- Cotini, S., Ripamonti, E., Caccianiga, A., et al. 2013, *MNRAS*, **431**, 2661
- Croton, D. J., Springel, V., White, S. D. M., et al. 2006, *MNRAS*, **365**, 11
- Croton, D. J., Stevens, A. R. H., Tonini, C., et al. 2016, *ApJS*, **222**, 22
- Cui, W., Springel, V., Yang, X., De Lucia, G., & Borgani, S. 2011, *MNRAS*, **416**, 2997
- Dariush, A., Khosroshahi, H. G., Ponman, T. J., et al. 2007, *MNRAS*, **382**, 433
- Dariush, A. A., Raychaudhury, S., Ponman, T. J., et al. 2010, *MNRAS*, **405**, 1873
- David, L. P., Nulsen, P. E. J., McNamara, B. R., et al. 2001, *ApJ*, **557**, 546
- Díaz-Giménez, E., Muriel, H., & Mendes de Oliveira, C. 2008, *A&A*, **490**, 965
- D’Onghia, E., Sommer-Larsen, J., Romeo, A. D., et al. 2005, *ApJL*, **630**, L109
- Driver, S. P., Hill, D. T., Kelvin, L. S., & Robotham, A. S. G. 2011, *MNRAS*, **419**, 971
- Dunlop, J. S., McLure, R. J., Kukula, M. J., et al. 2003, *MNRAS*, **340**, 1095
- Ellison, S. L., Patton, D. R., Mendel, J. T., & Scudder, J. M. 2011, *MNRAS*, **418**, 2043
- Fabian, A. C. 2012, *ARA&A*, **50**, 455
- Fabian, A. C., Sanders, J. S., Taylor, G. B., et al. 2006, *MNRAS*, **366**, 417
- Gabor, J. M., Impey, C. D., Jahnke, K., et al. 2009, *ApJ*, **691**, 705
- Gaspari, M., Brighenti, F., D’Ercole, A., & Melioli, C. 2011, *MNRAS*, **415**, 1549
- Gilkis, A., & Soker, N. 2012, *MNRAS*, **427**, 1482
- Gitti, M., Brighenti, F., & McNamara, B. R. 2012, *AdAst*, **2012E**, 6
- Gozaliasl, G., Finoguenov, A., Khosroshahi, H. G., et al. 2014, *A&A*, **566**, 140
- Graham, J., Fabian, A. C., & Sanders, J. S. 2008, *MNRAS*, **386**, 278
- Grogin, N. A., Conselice, C. J., Chatzichristou, E., et al. 2005, *ApJL*, **627**, L97
- Hlavacek-Larrondo, J., McDonald, M., Benson, B. A., et al. 2015, *ApJ*, **805**, 35
- Hopkins, A. M. 2013, *MNRAS*, **430**, 2047
- Jones, L. R., Ponman, T. J., & Forbes, D. A. 2000, *MNRAS*, **312**, 139
- Jones, L. R., Ponman, T. J., Horton, A., et al. 2003, *MNRAS*, **343**, 627
- Khosroshahi, H. G., Gozaliasl, G., Rasmussen, J., et al. 2014, *MNRAS*, **443**, 318
- Khosroshahi, H. G., Jones, L. R., & Ponman, T. J. 2004, *MNRAS*, **349**, 1240
- Khosroshahi, H. G., Maughan, B. J., Ponman, T. J., & Jones, L. R. 2006, *MNRAS*, **369**, 1211
- Khosroshahi, H. G., Ponman, T. J., & Jones, L. R. 2007, *MNRAS*, **377**, 595
- Kocevski, D. D., Faber, S. M., Mozena, M., et al. 2012, *ApJ*, **744**, 148
- Li, C., Kauffmann, G., Heckman, T. M., White, S. D. M., & Jing, Y. P. 2008, *MNRAS*, **385**, 1915
- Mauch, T., Klöckner, H.-R., Rawlings, S., et al. 2013, *MNRAS*, **435**, 650
- McNamara, B. R., & Nulsen, P. E. J. 2007, *ARA&A*, **45**, 117
- Miraghaei, H., Khosroshahi, H. G., Klöckner, H.-R., et al. 2014, *MNRAS*, **444**, 651
- Miraghaei, H., Khosroshahi, H. G., Sengupta, C., et al. 2015, *AJ*, **150**, 196
- Nulsen, P. E. J., Jones, C., Forman, W. R., et al. 2007, in *ESO Astrophys. Symp., Heating Versus Cooling in Galaxies and Clusters of Galaxies*, ed. H. Bohringer et al. (Berlin: Springer), **210**
- Peterson, J. R., & Fabian, A. C. 2006, *PhR*, **427**, 1
- Ponman, T. J., Allan, D. J., Jones, L. R., Merrifield, M., & MacHardy, I. M. 1994, *Natur*, **369**, 462
- Ramos Almeida, C., Tadhunter, C. N., Inskip, K. J., et al. 2011, *MNRAS*, **410**, 1550
- Randall, S. W., Nulsen, P. E. J., Jones, C., et al. 2015, *ApJ*, **805**, 112
- Raouf, M., Khosroshahi, H. G., & Dariush, A. 2016, *ApJ*, **824**, 140
- Raouf, M., Khosroshahi, H. G., Ponman, T. J., et al. 2014, *MNRAS*, **442**, 1578
- Raouf, M., Shabala, S. S., Croton, D. J., Khosroshahi, H. G., & Bernyk, M. 2017, *MNRAS*, submitted
- Robotham, A. 2010, *PASP*, **27**, 76
- Robotham, A. S. G., Norberg, P., Driver, S. P., et al. 2011, *MNRAS*, **416**, 2640
- Russell, D. M., Gallo, E., & Fender, R. P. 2013, *MNRAS*, **431**, 405
- Sabater, J., Best, P. N., & Argudo-Fernández, M. 2013, *MNRAS*, **430**, 638
- Sales, L. V., Navarro, J. F., Lambas, D. G., White, S. D. M., & Croton, D. J. 2007, *MNRAS*, **382**, 1901
- Sanchez, S. F., Jahnke, K., Wisotzki, L., et al. 2004b, *ApJ*, **614**, 586
- Sanderson, A. J. R., Edge, A. C., & Smith, G. P. 2009, *MNRAS*, **398**, 1698
- Schawinski, K., Simmons, B. D., Urry, C. M., Treister, E., & Glikman, E. 2012, *MNRAS*, **425**, L61
- Smith, G. P., Khosroshahi, H. G., Dariush, A., et al. 2010, *MNRAS*, **409**, 169
- Springel, V., White, S. D. M., Jenkins, A., et al. 2005, *Natur*, **435**, 629
- Tal, T., van Dokkum, P. G., Nelan, J., & Bezanson, R. 2009, *AJ*, **138**, 1417
- Taylor, E. N., Hopkins, A. M., Baldry, I. K., et al. 2011, *MNRAS*, **418**, 1587
- Vogelsberger, M., Genel, S., Springel, V., et al. 2014, *Natur*, **509**, 177
- Werner, N., Oonk, J. B. R., Sun, M., et al. 2014, *MNRAS*, **439**, 2291
- Zhuravleva, I., Churazov, E., Schekochihin, A. A., et al. 2014, *Natur*, **515**, 85